Electroanalytical Chemistry and Interfacial Electrochemistry
Elsevier Sequoia S.A., Lausanne – Printed in The Netherlands

THE STABILITY OF EMULSIONS*

DONALD R. WOODS and KENNETH A. BURRILL
Department of Chemical Engineering, McMaster University, Hamilton (Canada) and The van 't Hoff Laboratorium, Utrecht, (The Netherlands)

(Received 5th August 1971)

It is a pleasure to contribute a paper to this volume honoring Professor Overbeek. The stability of foams or emulsions and the properties of thin liquid films have long attracted his interest and that of his coworkers at the van 't Hoff Laboratorium[1–10].

The work described here considers the problem of the stability of emulsions. When two oil drops approach each other a thin film of the continuous water phase is trapped between the drops. The behavior of the thin film dictates whether the emulsion is stable or unstable; the rate of thinning of the film essentially determines the time required for the drops to coalesce. In the work reported here the rate of thinning of the film was studied for a free drop of oil rising through water to coalesce at a planar interface. To ensure that the film ruptured and to simplify the analysis, sufficient KCl was added to minimize the double layer repulsion. The objective was to identify the mechanisms of film drainage so that from these experiments on an idealized system of a single drop some insight might be gained into the stability of emulsions. The procedure was to observe the behavior, devise mechanisms to explain the behavior, where possible, to develop mathematical models based on the mechanisms and to evaluate the models.

A further objective of this paper is to illustrate how the equations describing the fluid dynamical behavior in the film can be linked with the equations describing surface behavior and to relate this work to the results of others.

1. EXPERIMENTAL OBSERVATIONS

The rest-times of the drops at the interface, τ, and the light interference patterns of the thin film (as viewed from above) were measured as a function of drop diameter, concentration of surfactant and the physical properties of the system. Drops of 2–4 mm diameter gave a reasonably large diameter of "contact" for the light interference studies yet the shape of the drop was essentially spherical. This last feature simplified the subsequent mathematical analysis.

Special techniques were developed to clean the bulk oil–water interface and to form drops of reproducible diameter. The drop rest-times were measured as an indirect function of interfacial concentration of surfactant by measuring directly the bulk concentration of surfactant and the interface age from the time of cleaning.

* Dedicated to Professor J. Th. G. Overbeek on the occasion of the 25th anniversary of his appointment as a Professor of Physical Chemistry.

The oils used in this study were toluene, anisole, cyclohexanol, and a mixture of cyclohexane and anisole (CA). Thus, the oil/water density difference was varied from 0.0097 to 0.133 gcm^{-3}, the interfacial tension from 3.93 to 35.0 mNm^{-1}, and the discontinuous oil phase viscosities from 0.59 to 32.8 cP, at 25° C. The aqueous phase concentration of the sodium lauryl sulfate (SLS) surfactant was varied from 0 to 10^{-2} gl^{-1} for the toluene/water system, and from 10^{-6} to 10^{-4} gl^{-1} for the other three systems. The volumes of the drops ranged from 0.001 to 0.020 ml for the four oil/water systems. Some experiments were done with 2-(2-ethoxyethoxy)ethanol as the surfactant. Details of the experimental technique and a description of the cell are given elsewhere[11].

The drop rest-times and the light interference patterns, produced by the thin film formed between the drop and bulk interfaces, were observed simultaneously. Consequently, the drop rest-time could be characterized by the additional observation of the distribution of film thicknesses during drainage as a function of radius and time. Indeed, sometimes the film drained unevenly or along one radial direction so that the patterns appeared as a series of ellipses rather than the concentric circle pattern observed when the drainage was even. The appearance of even or uneven film drainage for a particular drop was found to be a function of the interfacial concentration of the adsorbed surfactant.

Five distinct patterns in the type of film drainage were observed for different interfacial concentrations of adsorbed surfactant for the four oil/water systems studied.

First consider some typical data shown in Fig. 1 for the toluene/water system.

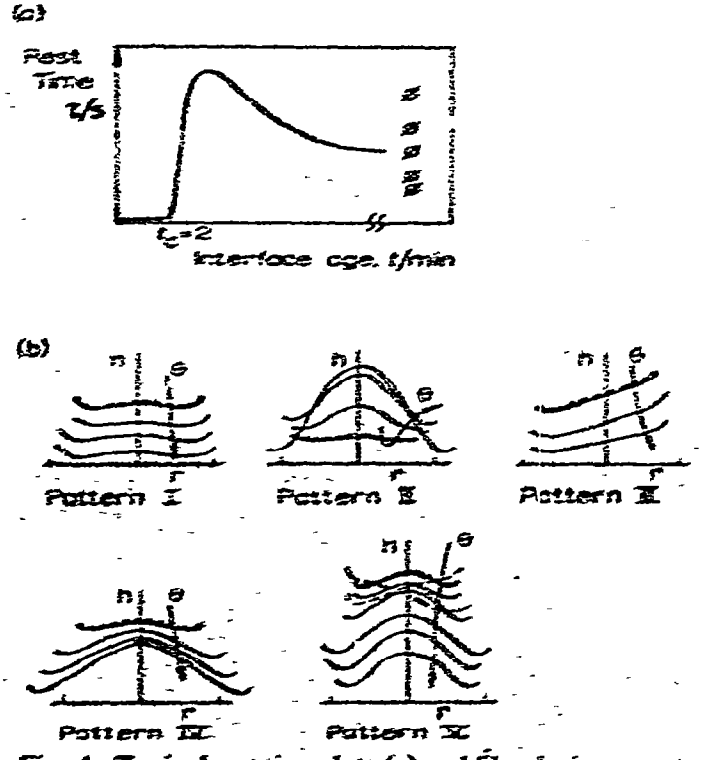

Fig. 1. Typical rest time data (a) and film drainage patterns (b).

The rest time, τ, is plotted *vs.* the age of the interface, t, for fixed bulk concentrations of surfactant, fixed diameter and for one system. (If we knew the rates of adsorption of surfactant, this could be plotted as τ *vs.* interfacial concentration, Γ. However, this is difficult to determine). If the bulk concentration is increased, the τ *vs.* t curve shifts to the left. These data show three distinct reproducible features: almost zero rest-time for $t < 2$ min, followed by a maximum rest-time, τ_{max}, and followed by a gradually decreasing rest-time. A fourth feature is a widely scattered rest-time when the interface was several hours old. Now let us combine the rest-time data with the light interference observations that were made simultaneously. Five distinctly different patterns of film behavior have been observed. Four of these have been described by Hodgson and Woods[11] for oils with low viscosity:

Pattern I

This was described as rapid, uniform thinning to coalescence and illustrated in their Fig. 7[11] and corresponds with the behavior for $t < 2$ min in Fig. 1.

Pattern II

This was described as rapid thinning to black, inflow to dimple and draining to coalescence and shown in their Fig. 8[11] and corresponds with the maximum rest-time conditions in Fig. 1.

Pattern III

Their Fig. 9 illustrates this unsymmetrical drainage[11] and sometimes occurs in the gradually decreasing rest-time trend in Fig. 1.

Pattern IV

This pattern, shown in their Fig. 10, they describe as slow dimpled drainage[11] and occurs as an alternative pattern in pattern III corresponding to the gradually decreasing rest-time trend in Fig. 1. The barrier ring radius or the radius corresponding to the thinnest film thickness, expands with elapsed time.

Pattern V

This has been observed by Burrill[12] for the viscous cyclohexanol drops in water. During the first 60 s of elapsed time, the film drainage alternated between even and uneven drainage. Then the drainage settled down to even drainage until rupture. The barrier ring radius decreased slightly with increased elapsed time. Some aspects of this are shown in the data of Robinson and Hartland[13] although their data suggest that the barrier ring radius is almost independent of elapsed time.

Each pattern is unique in that for any given age of the interface, t, there will be one specific pattern. In general, Hartland[14] seems to have observed most of these patterns for the 8–10 mm diameter drops that he studied in more viscous systems. By far the most common patterns are patterns III and IV. Patterns I and II occur only for interfaces that are relatively free of surfactant. An important question is when can one expect pattern III behavior and when, pattern IV? The experimental evidence is complex. Burrill[12] has found alternating regions of interface age, for a given bulk concentration, when the behavior would change from even to uneven drainage and then back to even drainage. That is, for a 0.0025 ml drop of CA in water with a bulk

concentration, c^1, of 10^{-6} g l^{-1} SLS, pattern IV behavior occurs for $t < 2$ min and pattern III behavior for $t > 4$ min. However, for higher bulk concentrations, $c^1 = 10^{-4}$, the reverse happens. Pattern III occurs for short interface ages and pattern IV at long interface ages. Detailed plots of the data are given elsewhere[12].

To put this phenomenon qualitatively into perspective these results for two different bulk concentrations can be combined by estimating the interfacial concentration of surfactant (alternatively a reference bulk concentration, the highest bulk concentration, can be used and the time, t, estimated when for the reference system the interfacial concentration equals that for various combinations of interface age and bulk concentration). When this is done the patterns alternate between patterns III and IV as the interfacial concentration increases. A summary of the observations for the variation in film thickness and the rest-times for the systems studied by Burrill[12] is given in Table 1.

Besides studying the variation in film thickness and the rest-times in order to understand the coalescence mechanisms, the circulation patterns in the bulk fluid phases bounding the trapped film can be studied. Naturally one hopes that the tracers added to make the circulation visible do not affect the phenomena being studied. Hartland[14] studied the circulation patterns with 0.025 mm lycopodium powder for fluid drops and with a non-uniform density rigid sphere for rigid non-deformable drops[15].

We now break down the observed patterns into mechanisms which can be used as the basis of theories for quantitatively predicting the observations.

2. MECHANISMS OF FILM DRAINAGE

Consider first the fundamental concepts and then the mechanisms.

2.1. *Fundamental concepts*

The fundamental concepts we can use to describe this system, in general, are as follows:

1. The drop rises because of buoyancy. Because it has a velocity and mass it also has inertia.

2. Water in the film can flow out of the film because of a radial pressure gradient and because of movement or mobility of the bounding interfaces.

3. Since both interfaces are fluid and can curve, pressure and curvature are related.

4. A non-uniform distribution of surfactant at the interface gives a gradient in the interfacial tension.

5. At any mobile, fluid interface there is continuity of the shear stress.

6. The interface will resist a shear stress so that the interfacial velocity is zero if there is sufficient surfactant in the interface to prevent lateral movement. We call this condition steric immobility (it is likely to be important when insoluble surfactants are present at the interface, or when the desorption of soluble surfactants is slow relative to the fluid dynamical interactions).

7. Water flowing out of the film sets up a shear stress at the bounding interfaces which causes the interfaces to be mobile unless the shear stress is everywhere balanced by an interfacial tension gradient. When such a balance occurs the interface can be called dynamically immobile.

J. Electroanal. Chem., 37 (1972)

TABLE 1 — SUMMARY OF REST-TIME DATA FOR ALL SYSTEMS, FOR 10^{-6} g l^{-1} SLS + KCl

Oil/water system	γ/mN m^{-1}	$\Delta\rho$/g cm^{-3}	μ_{oil}/cP	Drop volume/ml	Range of interface age $\tau < 1$ s 0-t_c/min	Interface age/min and τ_{max}/s: t	τ_{max}	Mode of drainage just after t_c	Mode of drainage changes at t_m (min) to:	Mode of drainage at t_x; av. rest-time, $\bar{\tau}_x$/s	Order of magnitude rest-time for range of interface age studied/s
a. Normality KCl = 0.01											
Toluene/water	35	0.133	0.59	0.005[a]	0-1	2	12	Even	—	Uneven $\bar{\tau}_x = 8$	10
Anisole/water	20.5	0.0097	1.32	0.005	0-2	4	15	Uneven	—	Uneven $\bar{\tau}_x = 1$	10
				0.010	0	2	27	Uneven	—	Uneven $\bar{\tau}_x = 2$	15
				0.020[a]	0	6	34	Even	Uneven $t_m = 3$	Uneven $\bar{\tau}_x = 5$	20
Cyclohexanol/ water	3.93	0.051	32.8	0.001[a]	0	3	110	Composite of even and uneven	—	Composite $\bar{\tau}_x = 40$	70
CA/water	28.9	0.053	0.85	0.0025	0	0		Even	Uneven $t_m = 2$	Uneven $\bar{\tau}_x = 3$	7
				0.005[a]	0	0	16	Even	Uneven $t_m = 4$	Uneven $\bar{\tau}_x = 4$	10
b. Normality KCl = 0.05											
Toluene/water				0.005	0	1	7	Even	Uneven $t_m = 1$	Uneven $\bar{\tau}_x = 2$	5
Anisole/water				0.005	0	1	8	Uneven	Even $t_m = 2$	Uneven $\bar{\tau}_x = 3$	2
				0.010	0	0	28	Uneven	Even $t_m = 4$	Uneven $\bar{\tau}_x = 8$	3
				0.020	0	0	31	Uneven	Even $t_m = 12$	Uneven $t_m = 10$	5
Cyclohexanol/ water				0.001	0	—	240 (no max.)	Composite of even and uneven drainage	—	Composite $\bar{\tau}_x = 195$	240
CA/water				0.0025	0	0	4	Uneven	Even $t_m = 2$	Uneven $\bar{\tau}_x = 1$	1
				0.005	0	0	6	Uneven	Even $t_m = 11$	Uneven $\bar{\tau}_x = 2$	2

[a] These drop volumes produce the same radius of the light interference pattern.

8. The pressure is zero at some radial distance R. For all radial positions $r < R$, the integral of the pressure times the area balances the force bringing the two interfaces together. If inertia, van der Waals and double layer repulsion are neglected, then the buoyant force is the force to be balanced by the pressure in the film. This is:

$$\Pi = Wg = \int_{r=0}^{r=R} 2\pi r p \, dr \tag{1}$$

where Π = disjoining pressure.

Consider now some calculations based on these concepts and experimental data. The distribution of surfactant at the interface for various sets of coalescence data can be estimated by the procedure outlined in Fig. 2.

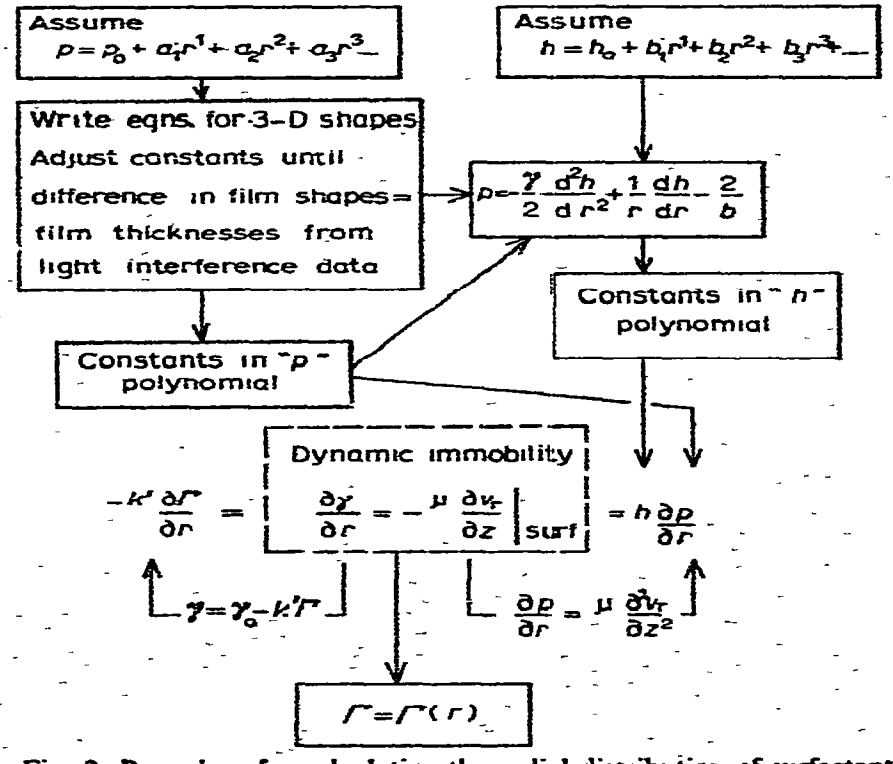

Fig. 2. Procedure for calculating the radial distribution of surfactant at the interface for conditions of dynamic immobility.

Assume the pressure distribution within the film to be polynomial in radial distance, r. The values of the constants are determined from fundamental (F8) in eqn. (1):

$$p = p_0 + a_2 r^2 + a_4 r^4 + a_6 r^6 \tag{2}$$

The condition of dynamic immobility requires that at the bulk interface $z = h$, the interfacial tension gradient $\partial\gamma/\partial r$ is equal to the shear stress at the interface. That is:

$$\frac{\partial \gamma}{\partial r} = -\mu \frac{\partial v_r}{\partial z}\Big|_{z=h} \tag{3}$$

The term on the l.h.s. can be related to the interfacial concentration, Γ, assuming the interfacial tension is given by:

$$\gamma = \gamma_0 - k^1 \Gamma \tag{4a}$$

or

$$\partial\gamma/\partial r = -k^1 \partial\Gamma/\partial r \tag{4b}$$

where γ_0 = interfacial tension when no surfactant is present in the interface or at some reference concentration in a region where eqn. (4) may be assumed to be valid; k^1 = constant.

The term on the r.h.s. can be related to the pressure *via* the equation of motion in the film. For isothermal, steady state, creeping flow conditions, neglecting gravitational effects, the equation is, in cylindrical coordinates:

$$\partial p/\partial r = \mu \partial^2 v_r/\partial z^2 \tag{5a}$$

Assuming the drop interface is mobile or the oil in the drop is inviscid, *i.e.* $\partial v_r/\partial z = 0$ at $z = 0$, yields

$$\mu \partial v_r/\partial z = z \partial p/\partial r \tag{5b}$$

For dynamic immobility, substitution of eqns. (4b) and (5b) into eqn. (3) gives:

$$-k^1 \frac{\partial \Gamma}{\partial r} = z \frac{\mathrm{d}p}{\mathrm{d}r}\bigg|_{z=h} = h \left(\frac{\mathrm{d}p}{\mathrm{d}r}\right)\bigg|_{z=h} \tag{6}$$

To determine the distribution of surfactant, values of both variables on the r.h.s. of eqn. (6) are needed, namely $z = h$ and p.

The method used is as follows. General equations are written in terms of the pressure in the film and the three-dimensional shapes of the interfaces bounding the film. This equation has an adjustable parameter R. A value of R is chosen such that the film thickness between the calculated three-dimensional shapes of the interfaces matches the film thickness observed in experimental light interference data for all radial locations. Details are given by Burrill and Woods[16]. Thus, the three-dimensional shapes and all the constants in the pressure polynomial can be calculated.

A key equation in this calculation is a simplified form of the Laplace equation:

$$p = \frac{-\gamma}{2}\left[\frac{\mathrm{d}^2 h}{\mathrm{d}r^2} + \frac{1}{r}\frac{\mathrm{d}h}{\mathrm{d}r} - \frac{2}{b}\right] \tag{7}$$

If we assume

$$h = h_0 + b_2 r^2 + b_4 r^4 + b_6 r^6 + b_8 r^8 \tag{8}$$

we can then use the appropriate derivatives of eqn. (8) in eqn. (7) and a term by term comparison with eqn. (2) yields values for the constants in eqn. (8). Then, the derivative of eqn. (2) with respect to r times eqn. (8) can be substituted into eqn. (6) and the resulting equation integrated with respect to r. For the sake of illustration we assume $\Gamma = \Gamma_0$ at $r = 0$ where $\Gamma_0 > 0$. The result is an expression for the radial distribution of surfactant at the interface

$$\Gamma = \Gamma_0 - \frac{2}{k^1} \sum_{\substack{i=2 \\ \text{even} \\ \text{numbers}}}^{14} \frac{c_i r^i}{i} \tag{9}$$

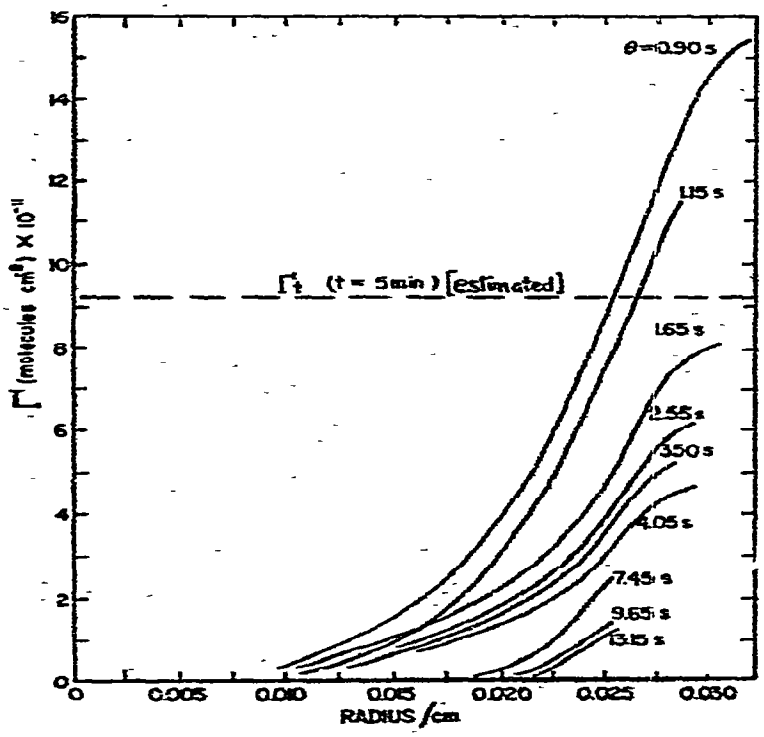

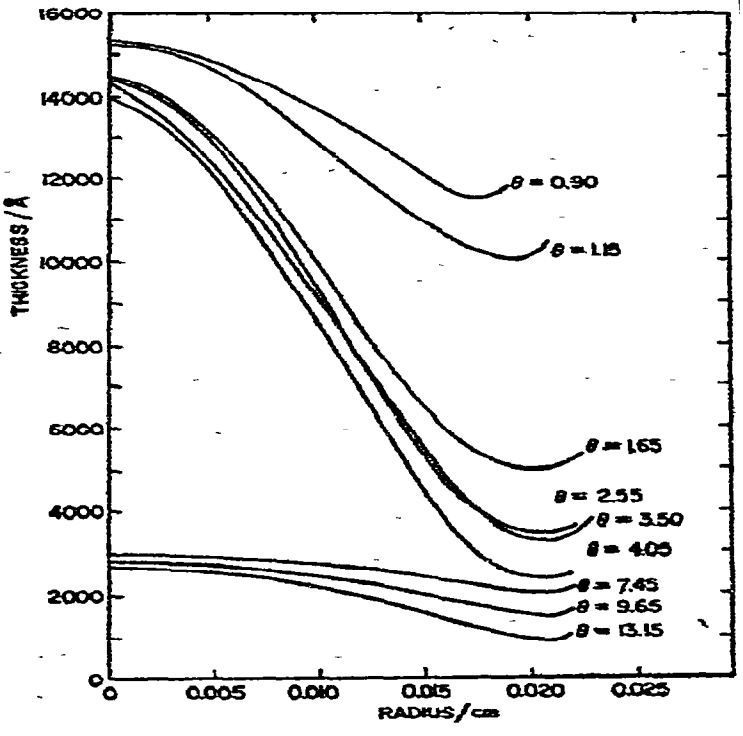

Fig. 3. Calcd. Γ as a function of radius for the film profiles in Fig. 4.

Fig. 4. Film thickness profiles of anisole drop, volume 0.020 ml, in water with 10^{-6} g l^{-1} SLS+0.01 N KCl (at $\theta > 4.05$ s, uneven profiles are approximated by even, symmetric profiles).

The results of such a calculation are shown in Fig. 3 for the film thickness profiles given in Fig. 4.

From these calculations we can add the fundamental concept that:

9. When dynamic immobility is or is being set up there exist distributions in both surfactant and interfacial tension that have their respective maximum, Γ_{max}, and minimum in the region $r^+ = r/R = 1$.

Thus, away from the region $r^+ = 1$, are both interfacial tension gradients that attempt to expand the interface and concentration driving forces $(\Gamma_{max} - \Gamma)$ and $(\Gamma_{max} - c^1)$ that encourage the surfactant to leave, by surface diffusion or desorption into the bulk.

10. The preceding concepts have been applied to describe the rise or fall of fluid drops through an infinite fluid. If there is negligible surfactant present, the surface of the drop is mobile and circulation occurs within the drop as illustrated in Fig. 5(a). If small amounts of surfactant are present, the surfactant is swept to the downstream part or rear of the drop and a surface tension gradient is set up along the drop surface that may or may not be sufficient to cause dynamic immobility. Such a distribution is shown in Fig. 5(b). This problem has been described extensively in the literature. See, for example, Levich[17], Linton and Sutherland[18] and Garner[19].

Consider now the mechanisms that make up the observed thinning phenomena and that are based on these fundamental concepts.

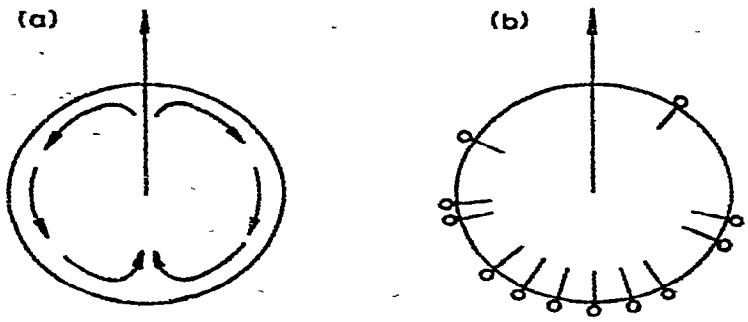

Fig. 5. Different interfacial conditions for a drop rising through an infinite fluid. (a) System free of surfactants; (b) distribution of surfactants along the interface of a rising drop.

2.2. *The mechanisms*

Each of the five patterns of behavior observed can be broken down into what might be called four fundamental types of behavior. The patterns are made up of the sequential or simultaneous occurrence of the different types of behaviour. The four types are:

1. rapid approach: outflow of fluid from the film occurs because the bounding interfaces are mobile and there is only a small radial pressure gradient.
2. dimple formation: inflow of fluid into the film because the interfacial tension gradient causes contraction of the interface and drags the bounding bulk fluid inwards.
3. even drainage: symmetrical outflow of fluid from the film because of a radial pressure gradient. At least one of the bounding interfaces is usually immobile.
4. uneven drainage: unsymmetrical outflow of fluid from the film because of local interfacial mobility aided by a radial pressure gradient.

Mechanisms can be proposed for these four types of behavior. The following are hypotheses that qualitatively explain the observations. The test of the hypotheses lies in how well the theoretical models based on the hypotheses predict the observations.

Rapid approach mechanism. Rapid approach is the outflow of fluid from the film with the bounding interfaces being mobile and with little radial pressure gradient within the barrier ring. The mechanism for this is relatively easy to explain. Because of its buoyancy, the drop approaches the bulk interface. A film forms between the drop and bulk interfaces and the decreasing thickness of the film begins to restrict the outward flow of liquid from the film. This restriction of flow is increased if the mobility of the bounding interfaces is reduced as a result of the viscosity of one of the bulk phases, because adsorbed surfactant is distributed along the interface and a significant interfacial tension gradient exists or because the interfaces are immobile as either the shear stress is everywhere balanced by an interfacial tension gradient, or the interfacial concentration of surfactant is so high that steric hindrance prevents lateral motion of the surfactant and the interface is immobile. If an interfacial tension gradient is set up, both the drop buoyancy force and the inertia force, which acts on the drop as it decelerates, do work on the bulk interface to set up this gradient. By doing work, the kinetic energy of the drop may be dissipated and replaced by surface energy. The drop buoyancy force is opposed by the pressure in the film which is set up by the restriction

of the efflux because of both the film thickness and the partial or complete immobility of the bulk interface.

The transfer of kinetic energy into the potential surface energy of an interfacial tension gradient is very rapid and, if complete, the period of rapid approach ceases. Initially, the bulk interface over-expands because the average film pressure necessary to balance both the buoyancy and inertia forces is larger than that necessary to balance just the buoyancy. If the transfer of the kinetic energy of the drop to the interfacial tension gradient cannot be completed because insufficient surfactant is adsorbed at the interface, then partial mobility of the bulk interface results, and film thinning continues rapidly until rupture.

Dimple formation mechanism. The mechanism begins when an interfacial tension gradient, caused by a distribution of surfactant at the interface, becomes greater than the shear stress acting on the interface. At this point in time, the interface contracts and the bulk interfacial velocity is directed toward the center of the film. The contracting interface drags the surrounding bulk fluid inwards into the film to form a dimple.

One way to obtain the prerequisites for dimple formation is for a drop to approach rapidly an interface containing a small amount of surfactant. When the drop is far from the bulk interface, there is no interfacial tension gradient, the surfactant is uniformly distributed along the interface and insufficient surfactant is there to resist the shear stress. During rapid approach, the shear stress at the interface causes the bulk interface to expand, sweeping surfactant with it. The distribution of surfactant, which can be calculated from eqn. (9), gives an interfacial tension gradient which balances the interfacial shear stress at all radial locations. The interface is then dynamically immobile (if there is insufficient surfactant to satisfy this distribution, then the shear stress exceeds the interfacial tension gradient and the interface is mobile, and rapid approach persists).

If there is sufficient surfactant, the distribution reaches a maximum Γ_{max} at $r = R$ with a corresponding minimum in the tension γ. Of more interest is the gradient of the interfacial tension and the shear stress, which are assumed to be equal. The shear stress arises because of the force contributions of both buoyancy and inertia. When the drop becomes arrested, the inertia contribution to the shear stress is lost. If the inertia of the drop becomes dissipated before the surfactant can redistribute itself at the interface, then the interfacial tension gradient exceeds the shear stress and dimple formation begins.

Another contribution that aids dimple formation occurs if there is surfactant present at the interface of the drop. Whether there is or not depends upon the procedure for forming the drop and the rates of adsorption. If surfactant is present, it will become distributed, as shown in Fig. 5(b), while it rises. Then, when the drop is arrested, there is an unbalanced interfacial tension gradient that causes interfacial movement from the rear of the drop toward the film. This movement could also promote dimple formation.

Even drainage mechanism. The fluid flows out of the film because of a radial pressure gradient. At least one of the bounding interfaces is in either dynamic or steric immobility.

This type of drainage is difficult to observe because often even drainage and dimple formation occur simultaneously. Indeed, sometimes, for example in pattern IV

behavior, these two simultaneous types of behaviour are such that the volume of fluid within the barrier ring is approximately independent of the elapsed time. Hence, to the observer it appears as though the thickness at the barrier ring decreases because of flow in the region beyond the barrier ring, *i.e.* $r > c$. Indeed, this was the basis for the simple model of Hodgson and Woods[11]. From a mechanistic viewpoint, this behavior at $r > c$ occurs because the pressure gradient is steeper in this region.

Uneven drainage mechanism. Uneven drainage, the unsymmetrical flow of fluid from the film because of local interfacial mobility aided by a pressure gradient, is caused because the local shear stress exceeds the interfacial tension gradient to cause local mobility of the bulk interface. Four possible causes of the local mobility are:

1. depleted dynamic immobility,
2. removal of local shear stress,
3. local impurities,
4. unsymmetrical circulation patterns.

For the most generally applicable cause: depleted dynamic immobility, Burrill[12] hypothesized that during the approach and the resultant dynamic immobility with its distribution of surfactant, the surfactant leaves the region of $r^+ = 1$ because of interfacial diffusion, desorption and radial interfacial tension gradients such that the supply of surfactant is locally depleted so that at a later elapsed time there is insufficient surfactant to balance the local shear stress. Uneven drainage begins. At the same time that Burrill was developing this theory Marucci[20] qualitatively described "the [desorption] diffusion controlled mechanism at the border of the film is believed to be the major cause of further thinning of the film down to rupture". Burrill believes this mechanism is the reason for uneven drainage and provided a quantitative analysis of the surfactant distribution and the order-of-magnitude estimation of the driving forces.

The second mechanism is important when the interfacial concentration Γ_t is small. Here, the sudden removal of some shear stress (for example, caused by the drop sliding laterally along the bulk interface) leaves a momentary distribution of surfactant that cannot be symmetrically redistributed before local mobility occurs along the line of former slide.

Particularly when the interface has aged for a long time, mixtures of surfactants in the region $r^+ = 1$ can cause local surface tension gradients that give local mobility. For example, when Burrill had his system as clean as possible, all the film drainage was uneven for all interface ages. When 10^{-6} g l^{-1} of SLS was added, the film drainage was even until the interface had aged several hours. There seemed to be no predictable radial direction along which uneven drainage occurred and no predictable rest time. This would agree with the hypothesis of mixed surfactants distributed throughout the bulk surface. Uneven drainage would occur whenever a large enough local interfacial tension gradient occurred near $r^+ = 1$.

Hartland[14] suggested that uneven drainage occurs in fluid–fluid systems because of the persistence of circulation within some portion of the fluid drop.

3. THEORETICAL PREDICTION OF EVEN FILM THINNING

Mathematical models should now be developed to test the hypotheses and to predict film thinning. The generalized equations to be solved to predict the film

thinning behavior include the macroscopic mass, force and energy balances, and the microscopic equations of change for the bulk fluids (drop, bulk oil phase I and in the continuous phase II) and for the two interfaces. The equations are linked by boundary conditions (such as those described in Section 2), flux expressions and equations of state. The main equations are summarized in Table 2. The complete set of equations, given in Table 2, is extremely complex and difficult to solve. Indeed, some very simple approximations to the complex problem have been useful and are widely used although, understandably, the predictions based on these models are often in error.

TABLE 2

OVERALL SET OF EQUATIONS TO BE SOLVED TO DESCRIBE FILM THINNING

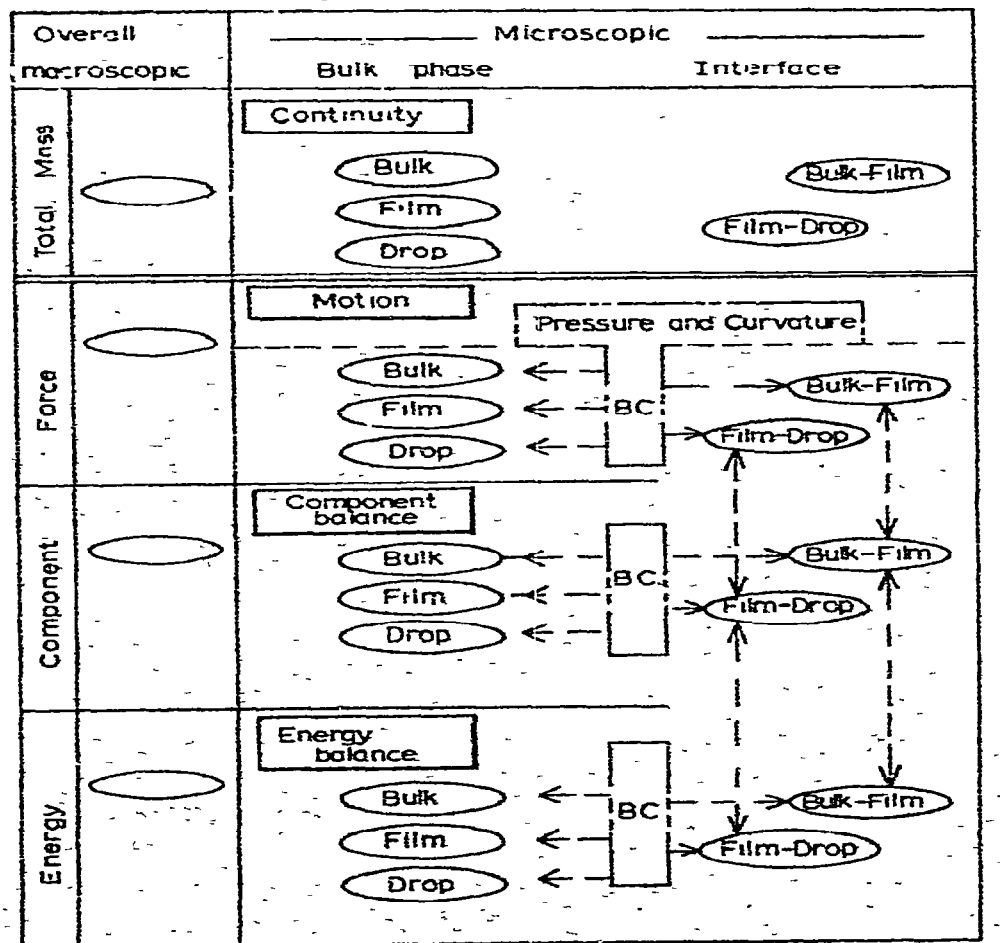

The easiest to describe is even drainage. For spherical drops at the interface it is usually satisfactory to assume that the coordinate system is cylindrical. For larger, non-spherical drops the spherical coordinate system is used. In this discussion we limit ourselves to the models developed in cylindrical coordinates. Hartland[21] has developed models to describe the behavior of larger drops where spherical coordinates are required. Most of his analysis is for even drainage and when the relative interface shapes are approximately equilibrium shapes. Thus, from these data[14] we can see that such an analysis should apply after the first 50 s of elapsed time.

Consider briefly some different sets of equations and what they predict.

A very popular approximation is the parallel discs model, solved by Stefan[22], Reynolds[23] and Taylor[24], and the various variations of it proposed by Charles *et al.*[25], Elton and Picknett[26], and Frankel and Mysels[27]. The set of equations solved is shown in Table 3. It should be noted that in solving this set of equations inconsistent assumptions are used. In this model, the main assumption is that both interfaces are immobile, and the distance of separation does not vary with radius, *i.e.* $\partial h/\partial r = 0$.

TABLE 3

PARALLEL DISCS MODEL

	Overall macroscopic	Microscopic: Bulk phase	Microscopic: Interface
Total Mass		Continuity: $\frac{\partial v_r}{\partial r} + \frac{v_r}{r} + \frac{\partial v_z}{\partial z} = 0$	
Force	$Wg = \int_0^R 2\pi r p\, dr$	Motion: $\frac{1}{\mu}\frac{\partial p}{\partial r} = \frac{\partial^2 v_r}{\partial z^2}$; $v_r = 0$; $v_r = 0$	$p_o = \text{const}$; $\frac{dh}{dr} = 0$; $p_o = \frac{2\gamma}{b}$

Generalized result for $p_o = \frac{k\gamma}{b}$ and $R^2 = \frac{HWg}{\pi p_o}$

$$\frac{dh}{d\theta} = \frac{-1}{2}\frac{k^2}{H^2}\left[\frac{\gamma^2}{\mu \Delta\rho g b^5}\right] h^3$$

$$\theta_2 - \theta_1 = \frac{H^2}{k^2}\left[\frac{\mu \Delta\rho g b^5}{\gamma^2}\right]\left[\frac{1}{h_2^2} - \frac{1}{h_1^2}\right]$$

This gives the result for the change in shape of the interface and the changes at both the barrier ring and at the center to be:

$$\frac{dh}{d\theta} = -\frac{\varepsilon}{6\mu} h^3 \qquad (10)$$

where h = thickness of the film, θ = time, $\varepsilon = 4Wg/\pi R^4 = 3p_0^2/H^2 g \Delta\rho b^3$, μ = viscosity of the fluid in the film, Wg = force bringing the drop and bulk together, $= \Delta\rho Vg$, R = radial location where the pressure in the continuous phase is zero, $\Delta\rho$ = density difference between the dispersed and continuous fluids, V = volume of the drop, b = radius of a spherical drop, p_0 = pressure at the center of the film at $r = 0$, $H = 1$ if

the pressure is assumed uniformly p_0 for $0 < r < R$, and 2 if the radial pressure distribution is assumed to be parabolic.

We note that values of R can be calculated from:

$$R^2 = HWg/\pi p_0 \tag{11}$$

The inconsistency in the model is that there is a parabolic pressure distribution in the film to cause the fluid to move out of the film, given by:

$$p = -\frac{\varepsilon}{2}(r^2 - R^2) \tag{12}$$

$$p = 2p_0((r^+)^2 - 1)$$

Yet because the materials bounding the film are fluids, there must be a variation in curvature; *i.e.*, $\partial h/\partial r \neq 0$. In other words, the geometry of parallel discs requires no pressure gradient in the film yet to expel fluid from the film trapped between immobile interfaces there must be a pressure gradient (and one is used to predict $dh/d\theta$). Thus from a geometric viewpoint the value should be $H = 1$ yet from a fluid dynamical viewpoint the value should be $H = 2$.

The pressure at the center of the film is given by

$$p_0 = 2\gamma/r_2 = k\gamma/b \tag{13}$$

where r_2 = equal principal radii of curvature of the bulk interface at the center of the film and k is $2b/r_2$. Chappelear[28] suggested that $r_2 = 2b$ whereas some authors use $r_2 = b$. Substitution of the appropriate information into eqn. (10) yields:

$$-\frac{dh}{d\theta} = \frac{1}{2}\left(\frac{k}{H}\right)^2\left(\frac{\gamma^2}{\mu\Delta\rho g b^5}\right)h^3 \tag{14}$$

and

$$\tau = \theta_2 - \theta_1 = \left(\frac{H}{k}\right)^2\left(\frac{\mu\Delta\rho g b^5}{\gamma^2}\right)\left(\frac{1}{h_2^2} - \frac{1}{h_1^2}\right) \tag{15}$$

TABLE 4

FRANKEL AND MYSELS' MODEL (1962)

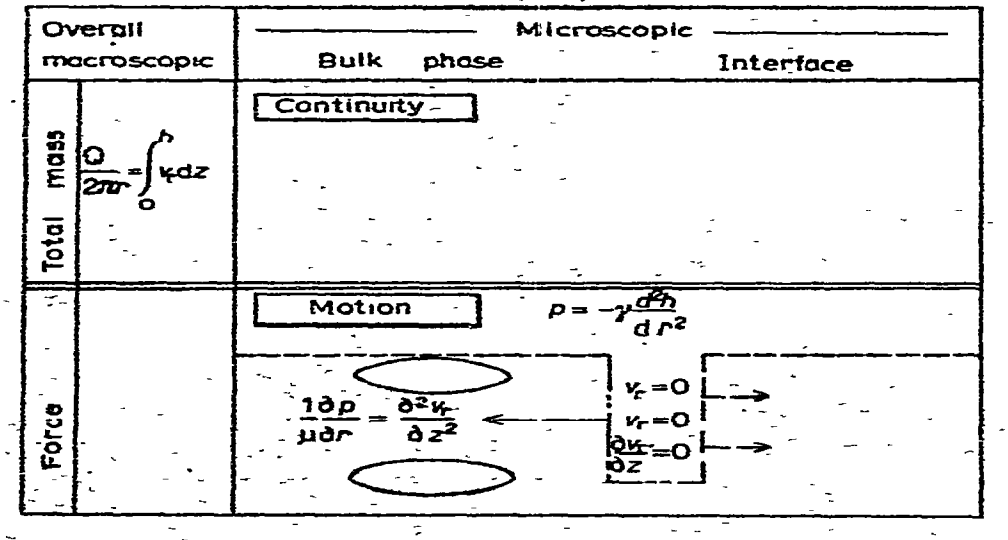

As a sidenote, these equations can be solved for the boundary condition that either the drop or the bulk interface is mobile, called $m=1$, *i.e.*, say at $z=0$, $\partial y_r/\partial z=0$.

The results are then:

$$\frac{-dh}{d\theta}=\frac{2}{3}\frac{\varepsilon}{\mu}h^3=\left(\frac{3-m}{3m}\right)\frac{\varepsilon}{\mu}h^3 \tag{16}$$

$$=\left(\frac{3-m}{m}\right)\left(\frac{k}{H}\right)^2\left(\frac{\gamma^2}{\mu\Delta\rho gb^5}\right)h^3 \tag{17}$$

where m = number of immobile interfaces. For $m=2$ we obtain eqn. (14). That is, the interfaces approach each other four times faster than if both interfaces are immobile.

Frankel and Mysels[27] allowed for the curvature of the interface and used a Laplace type expression for the pressure distribution as shown in Table 4. Their results were calculated by computer and the answers are not easy to represent simply. They cite the results for thinning at the center and at the barrier ring to be: at the center:

$$\tau=\theta_2-\theta_1=0.0027\left(\frac{2m}{3-m}\right)\left(\frac{\mu\Delta\rho gb^5}{\gamma^2}\right)\left(\frac{\Delta\rho gb^3}{\gamma}\right)^2\left(\frac{1}{(h_0^4)_2}-\frac{1}{(h_0^4)_1}\right) \tag{18}$$

at the barrier ring:

$$\tau=\theta_2-\theta_1=0.060\left(\frac{2m}{3-m}\right)\left(\frac{\mu\Delta\rho gb^5}{\gamma^2}\right)\left(\frac{1}{(h_c^2)_2}-\frac{1}{(h_c^2)_1}\right) \tag{19}$$

A simplified two-dimensional analysis of pattern IV behavior has been given by Hodgson and Woods[11] for the set of equations shown in Table 5. They assume that the volume of the film trapped inside the barrier ring is stagnant with an equilibrium pressure of $p_c=2\gamma/r_2$. The fluid flows from the film for $r>c$ because of a pressure gradient between a drop interface of radius r_3 and the flat bulk interface of radius r_2. The result is:

$$\frac{-dh}{d\theta}=\frac{\gamma}{3\mu r_2 r_3}h^2 \tag{20}$$

and

$$\tau=\theta_2-\theta_1=\frac{3\mu r_2 r_3}{\gamma}\left(\frac{1}{h_2}-\frac{1}{h_1}\right) \tag{21}$$

Hodgson and Woods[11] suggested that reasonable values of the radii of curvature are: $r_2=2b$, $r_3=b$.

Burrill[12] later suggested, based on calculations of the three-dimensional interface shapes from a polynomial distribution of the pressure, that $r_2=4b$ and $r_3=b$ or $p_c=\gamma/2b$. (For the pressure at the center of the film, he found $p_0=\gamma/b$.)

The approach of a rigid sphere approaching a rigid interface has been approximated by Charles and Mason[29] by the approach of a parabola of the same radius of curvature at the apex. The equations solved are summarized in Table 6. The result is:

$$\frac{-dh}{d\theta}=\frac{2}{9}\frac{\Delta\rho gbh}{\mu} \tag{22}$$

TABLE 5

HODGSON AND WOODS' MODEL (1969)

Overall macroscopic		Microscopic: Bulk phase	Microscopic: Interface
Total mass	$\frac{\partial Q}{\partial x} = \int_0^h v_x \, dz$	Continuity	
Force		Motion	$p_c = \frac{2\gamma}{r_2}$ $\quad h = h_c + \frac{(x-c)^2}{2r_3}$ $\frac{1}{\mu}\frac{\partial p}{\partial x} = \frac{\partial^2 v_x}{\partial z^2}$ $v_x = 0$ $v_x = 0$

$$-\frac{dh}{d\theta} = \frac{\gamma}{3\mu r_2 r_3} h_c^2$$

$$\theta_2 - \theta_1 = \frac{3\mu r_2 r_3}{\gamma} \left[\frac{1}{h_2} - \frac{1}{h_1} \right]$$

TABLE 6

RIGID PARABOLA (SPHERE) MODEL; CHARLES AND MASON (1960)

Overall macroscopic		Microscopic: Bulk phase	Microscopic: Interface
Total mass		Continuity $\frac{dv_r}{dr} + \frac{v_r}{r} + \frac{dv_z}{dz} = 0$	
Force	$Wg = \int_0^R 2\pi r p \, dr$	Motion	$h = h_o + \frac{r^2}{2b}$ $\frac{1}{\mu}\frac{\partial p}{\partial r} = \frac{\partial^2 v_r}{\partial z^2}$ $v_r = 0$ $v_r = 0$

and

$$\theta_2 - \theta_1 = \frac{9}{2}\left(\frac{\mu}{\Delta\rho g}\right)\frac{1}{b}\ln\frac{h_1}{h_2} \tag{23}$$

Brenner[30] and Maude[31] have solved the problem for a sphere and for the region of interest, namely thin films, MacKay *et al.*[32] have shown that the approximation used in eqns. (22) and (23) is reasonable.

An analysis that attempts to account for the effect of surfactant in the interface is based on the set of equations given in Table 7. This approach retains the assumptions of a parabolic radial pressure profile but allows for variation in h indirectly through the boundary $v_r = U$. The solution of this set of equations is an expression for the thickness of the film as a function of radial location:

$$\frac{\partial h}{\partial \theta} = -\frac{2}{3}\frac{\varepsilon}{\mu}h^3\left[2-\exp(-n'h)\right] + \frac{\varepsilon^2 R^2 h^4}{3\mu k^1 \Gamma_R}\exp(-n'h) \tag{24}$$

where $n' = \varepsilon r^2/2k^1\Gamma_R$. The results were reported by Burrill[12] for $p_0 = \gamma/b$ and for both $H=1$ and $H=2$.

TABLE 7

COUPLED PARALLEL DISCS MODEL; BURRILL AND WOODS (1971)

	Overall macroscopic	Microscopic: Bulk phase	Microscopic: Interface
Total mass		Continuity: $\frac{\partial v_r}{\partial r} + \frac{v_r}{r} + \frac{\partial v_z}{\partial z} = 0$	
Force	$Wg = \int_0^R 2\pi r p\,dr$	Motion: $\frac{1}{\mu}\frac{\partial p}{\partial r} = \frac{\partial^2 v_r}{\partial z^2}$; $p = p_0 2(r^{*2}-1)$; $p = p_0$; $\frac{dh}{dr} = 0$; $p_0 = \frac{\gamma}{b}$; $v_r = U$; $\frac{\partial v_r}{\partial z} = 0$	$-\mu\frac{\partial v_r}{\partial z}\Big\| = \frac{\partial \gamma}{\partial r}$; $\gamma = \gamma_0 - k'\Gamma$
Component		Component balance	$\frac{\partial \Gamma}{\partial \theta} = \frac{1}{r}\frac{\partial \Gamma U r}{\partial r}$

$$-\frac{\partial h}{\partial \theta} = \frac{2}{3}\frac{\varepsilon h^3}{\mu}\left[2-\exp(-nh)\right] - \frac{\varepsilon^2 R^2 h^4}{3\mu k'\Gamma_R}\exp(-nh)$$

$$n = \frac{\varepsilon r^2}{2k'\Gamma_R}$$

If Γ_R is small, then the equation becomes similar to the parallel discs model except that the pertinent expressions are

$\partial h/\partial\theta = -\varepsilon h^3/6\mu = -\alpha h^3$ $m=2$ both interfaces immobile

$\partial h/\partial\theta = -4\,\alpha h^3$ $m=1$ with one interface immobile

$\partial h/\partial\theta = -8\,\alpha h^3$ drop interface mobile; bulk interface moves with U and $\Gamma_R=0$

A final example of how the equations might be linked together to describe film thinning is shown in Table 8. Details of this model and of the results are given by Burrill[1,2].

TABLE 8

EXPONENTIAL PRESSURE DISTRIBUTION MODEL; BURRILL AND WOODS (1971)

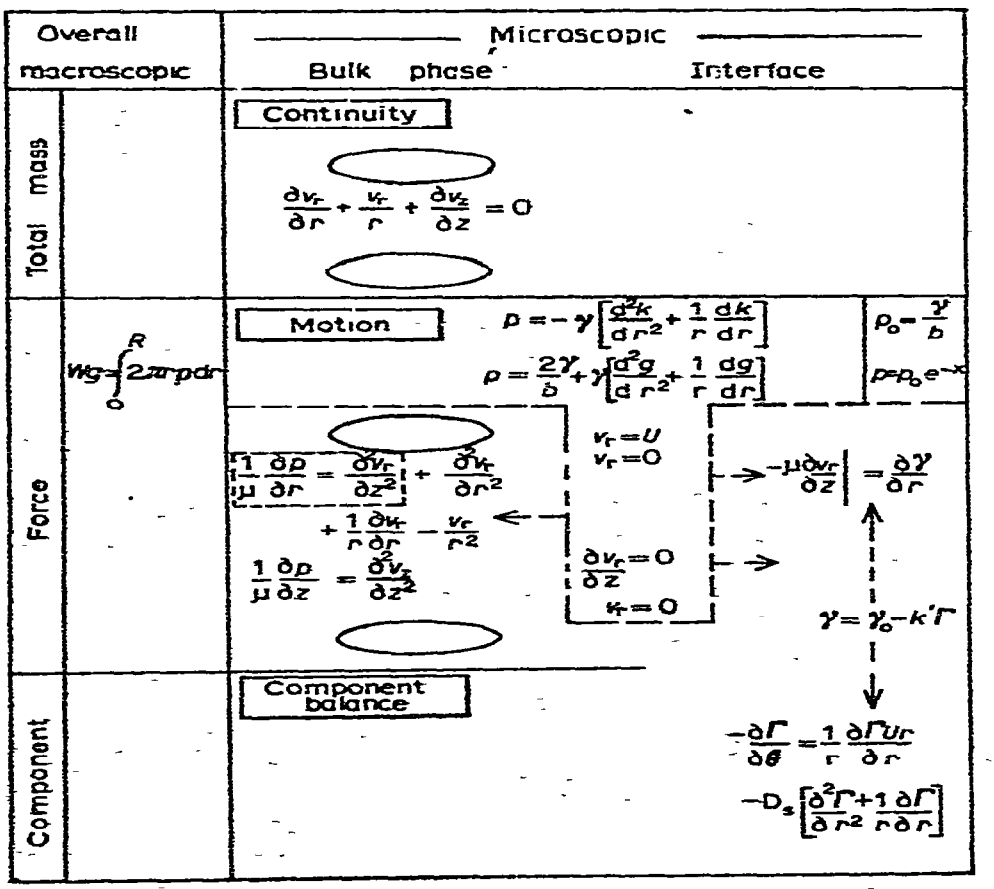

4. COMPARISON OF THEORETICAL PREDICTIONS WITH DATA

Ideally we want to be able to predict the shapes of the interfaces at any value of r and θ for any physical system. If this proves too difficult, then we want to predict:

— the rate of thinning of the barrier ring, $\partial h_c/\partial\theta$,

— the effect of the properties of the system on the rate of thinning of the barrier ring.

We can appreciate from the variety of mechanisms and drainage behavior that different models have to be used for different behavior. Furthermore, it is realistic to compare data and theory only when we have some confidence that the mechanisms governing both are similar.

As an expedient many authors average their rest-time data and report distributions of rest-times. This is usually done when the interface age, or alternatively the concentration at the interface, was not included as a control or measured variable. The averaging groups together data whose controlling mechanisms are most likely very different. For this reason, such data should not be used to test mechanisms and models unless it is known that the mechanisms for the model and the data are the same.

4.1. *Prediction of the shapes of the interfaces*

For pseudo-steady state conditions the shapes of the interfaces can be calculated from two-dimensional light interference data following the method of Burrill and Woods[16].

The relative shapes, or thickness profiles, for dynamic conditions calculated from the models in Tables 3 and 5 are not a function of r. From the data this is unrealistic. No evidence seems to have been reported of a comparison of the profiles predicted from the Frankel and Mysels model, Table 4, and experimental data.

The models described in Tables 7 and 8 should be applicable to all symmetrical mechanisms but do not adequately predict the variations in thickness profiles with time although they are an improvement over the parallel discs model.

The coupled model, Table 7, describes the formation of a dimple, and the shape and rate of formation is in good agreement with the data for anisole and toluene for one set of conditions. The prediction of the effects of interfacial concentration show the opposite trend to what is observed but the prediction of the effect of the height of arrest upon dimple formation shows the correct trend. The exponential pressure model, on the other hand, does not predict shapes that are reasonable. The effect of diffusion seems reasonable but, in general, the predicted rate of dimple deflation is too

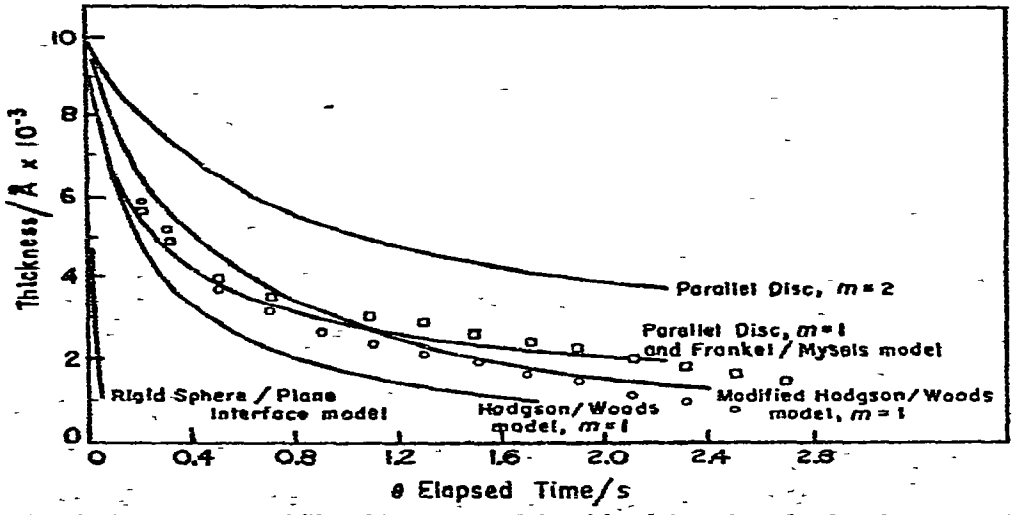

Fig. 6. Comparison of film thinning models with typical data for barrier ring thinning, toluene in water with 0.005 ml drop. $h_0 = 1 \times 10^{-4}$ cm for all models except the model of Frankel and Mysels.

large. Even for the viscous system, the predicted rate of thinning is about 100 times too fast. A redeeming feature of the equations used in this model is that a term-by-term analysis of the equations suggests that if the film thinning is dictated by behavior at or within the barrier ring then eqn. (14) is likely to dominate whereas eqn. (20) becomes dominant if the thinning is dictated by the fluid dynamics beyond the barrier ring.

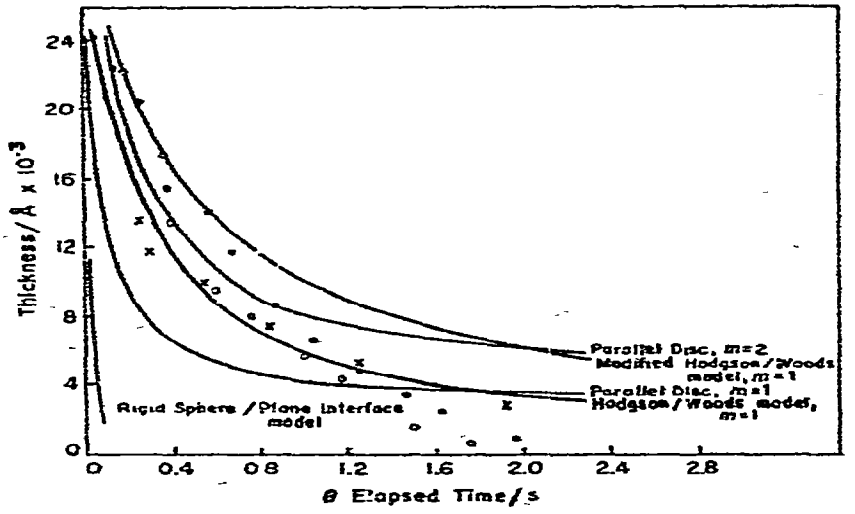

Fig. 7. Comparison of film thinning models with typical data for barrier ring thinning, anisole/water with $h_0 = 3 \times 10^{-4}$ cm for all models except $h_0 = \infty$ for parallel discs. Drop volume 0.020 ml; 10^{-4} g l^{-1} SLS + 0.05 *N* KCl; (×) t = 11 min; (○) t = 19 min; (●) t = 20 min.

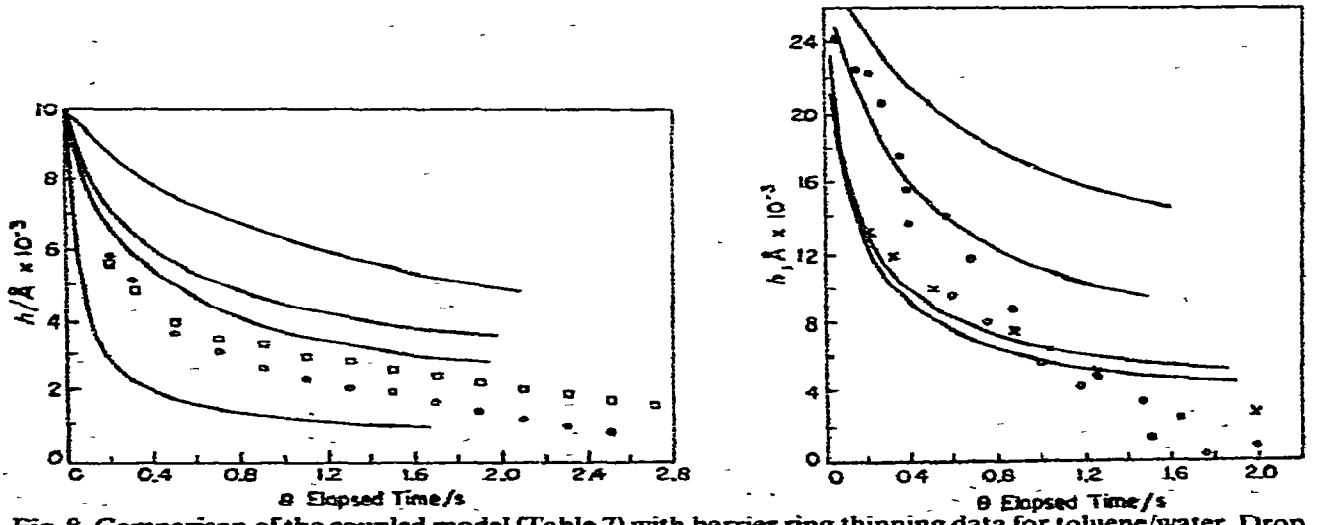

Fig. 8. Comparison of the coupled model (Table 7) with barrier ring thinning data for toluene/water. Drop volume 0.005 ml with $p_0 = \gamma/b = 330$ mN m^{-1} and $h_0 = 1.0 \times 10^{-4}$ cm. (——) Calculated from eqn. (24) for different values of $k'\Gamma_\infty$ and H.

Fig. 9. Comparison of the coupled model (Table 7) with barrier ring thinning data for anisole/water with drop volume 0.020 ml for $p_0 = \gamma/b = 120$ mN m^{-1} and $h_0 = 3.0 \times 10^{-4}$ cm. (——) Calcd. from eqn. (24) for different values for $k'\Gamma_\infty$ and H.

4.2. *Prediction of the rate of thinning at the barrier ring*

A comparison of the models and data where the even drainage mechanism or simultaneous even drainage and dimple formation mechanisms dominate is shown in Figs. 6–9. It is important that the theories agree with the data until a thickness of about 500Å for most oil–water systems. At this thickness rupture occurs, and the theory of Vrij and Overbeek[10] can be used to predict this phenomena for each specific problem. Thus models are sought that predict a continuing decrease in thickness. Agreement between the theory and the data is better for the toluene–water system than for the anisole–water system.

4.3. *Prediction of the effect of the variables on rest-times*

The effect of diameter and the physical properties has been studied by many workers. The effect of temperature has not received much attention. Jeffreys and Hawksley[33] studied the effect of temperature on the half-life of distributions of rest times and Lawson[34] suggested that the effect could adequately be described by the effect of temperature on the physical properties. No mechanism for film thinning was identified. The wide scatter of their data suggests that either the data that are averaged are controlled by different mechanisms or that there is mixed surfactant at the interface and uneven drainage controls.

No work seems to have been reported on the effect of temperature on even thinning. Consider first the effect of diameter. Table 9 shows values of the exponent n for the equation

$$\tau \simeq \beta b^n \tag{25}$$

TABLE 9

DEPENDENCE OF REST-TIME ON DROP RADIUS, $\tau \simeq \beta b^n$ BASED ON OBSERVED DATA

Oil/water system	*Diameter range/cm*	*n*	
		Even drainage	*Uneven drainage*
Anisole/water	0.1061–0.1682	1.1–2.4	1.6–2.5
CA/water	0.0842–0.1340	—	0.6
Cyclohexanol/water	0.0457–0.0620	1.9	2.9

TABLE 10

COMPARISON OF PREDICTED AND OBSERVED REST-TIMES BASED ON TOLUENE–WATER, EVEN DRAINAGE WITH 10^{-6} g l^{-1} SLS and $t = 5$ min

Oil/water system	*b/cm*	*m*	τ_{obs} /s	*Hodgson-Woods model*		*Parallel disc model*	
				τ_{pred} /s	% *diff.*	τ_{pred} /s	% *diff.*
Toluene/water	0.1061	1	8	—	—	—	—
Anisole/water	0.1682	1	28	34	+22	17	−39
CA/water	0.0842	1	5	6.4	+28	1.5	−70
Cyclohexanol/water	0.0620	2	90	97	+8	33	−64

when even drainage or even drainage with simultaneous dimple formation occur.

Theoretical values of $n=1$, 2 or 5 are predicted by the rigid-sphere, Hodgson and Woods or the parallel discs models respectively. These data suggest that the exponent is close to 2.

For the effect of physical properties of density difference and surface tension for low viscosity oil–water systems (and only for limited data for viscous oil phase, non-viscous film) Burrill[12] has shown that the two models, the parallel discs and Hodgson and Woods, bracket the actual data for even drainage. These results are shown in Table 10 where the toluene–water data are taken as base data and the rest-times for the three other systems are calculated from them.

ACKNOWLEDGEMENTS

The original research summarized in this paper was financed by the National Research Council of Canada. This paper was written while D. R. Woods was on a leave of absence from McMaster University and at the van 't Hoff Laboratorium in Utrecht. D. R. Woods was financially supported by a C. D. Howe Memorial Fellowship.

SUMMARY

Recent work on the film thinning behavior during the coalescence of oil drops in water is summarized. In the experimental work, color movies were taken of the light interference patterns produced by the thin film of water trapped between the rising drop and the bulk oil phase. The drops were relatively small (0.2–0.32 cm diam.); sufficient KCl was added to minimize double layer repulsion. Concentrations of 10^{-6}–10^{-2} g l^{-1} of sodium lauryl sulfate were used. The oils used were toluene, anisole, cyclohexanol and a mixture of anisole and cyclohexane.

Five different patterns of film behavior were observed. The mechanisms to explain these patterns are based on concepts of dynamic immobility (when the distribution of surfactant along the interface gives an interfacial tension gradient that everywhere balances the interfacial shear stress) and of steric immobility. The mechanisms include rapid approach (when both interfaces are mobile), dimple formation (when the interfacial tension gradient exceeds the interfacial shear stress), even drainage (when the interfaces are dynamically or sterically immobile) and uneven drainage (when there is local mobility). Reasons for uneven drainage are discussed.

The different theoretical models developed to describe film thinning are reviewed. The emphasis is on the assumptions and the relationship between the equations describing flow in the film and those describing surface behavior.

The predictions of the different models are compared but the emphasis is on the success of more recent models based on the above mentioned mechanisms to describe symmetrical film drainage.

REFERENCES

1 J. Th. G. Overbeek in H. R. Kruyt (Ed.), *Colloid Science, Vol. I: Irreversible systems*, Elsevier, Amsterdam, 1952, chaps. 2, 6 and 7.

2 E. J. W. Verwey and J. Th. G. Overbeek, *Theory of the Stability of Lyophobic Colloids*, Elsevier, Amsterdam, 1948.
3 A. J. de Vries, *Foam Stability*, Dissertation, van 't Hoff Laboratorium, Utrecht, 1957; *Rec. Trav. Chim.*, 77 (1958) 81, 209, 283, 383, 441.
4 W. Albers and J. Th. G. Overbeek, *J. Colloid Sci.*, 14 (1959) 501, 510; 15 (1960) 489.
5 J. Th. G. Overbeek, *J. Phys. Chem.*, 64 (1960) 1178.
6 E. H. Lucassen-Reynders, *Stabilization of Water in Oil Emulsions by Solid Particles*, Dissertation, van 't Hoff Laboratorium, Utrecht, 1962.
7 E. M. Duyvis, *The Equilibrium Thickness of Free Liquid Films*, Dissertation, van 't Hoff Laboratorium, Utrecht, 1962; E. M. Duyvis and J. Th. G. Overbeek, *K. Ned. Akad. Wet., Proc. Ser. B*, 65 (1962) 26.
8 R. C. Groot, *The Ultracentrifugation of Oil in Water Emulsions*, Dissertation, van 't Hoff Laboratorium, Utrecht, 1959; *K. Vlaam. Acad. Wet., Lett. Schone Kunsten Belg. Jaarb., spec. edn.*, (1966) 172.
9 J. Th. G. Overbeek, *Proc. IV. Int. Congr. Surf. Act. Subst., Brussels, September*, 1964, *Vol. II*, sect. B. Gordon and Breach, London, 1967, pp. 19–37.
10 A. Vrij and J. Th. G. Overbeek, *J. Amer. Chem. Soc.*, 90 (1968) 3074.
11 T. D. Hodgson and D. R. Woods, *J. Colloid Interfacial Sci.*, 30 (1969) 429.
12 K. A. Burrill, *PhD. Thesis*, McMaster University, Hamilton, Canada, 1970.
13 D. Robinson and S. Hartland, *Chem. Eng. J.*, 1 (1970) 22.
14 S. Hartland, *Chem. Eng. Sci.*, 24 (1969) 611.
15 S. Hartland and D. Robinson, *Chem. Eng. Sci.*, 25 (1970) 277.
16 K. A. Burrill and D. R. Woods, *J. Colloid Interfacial Sci.*, 30 (1969) 511.
17 V. G. Levich, *Physicochemical Hydrodynamics*, Prentice-Hall, Englewood Cliffs, New Jersey, 1962.
18 M. Linton and K. L. Sutherland, *Proc. II. Int. Congr. Surf. Act. Lond., Vol. I*, Butterworths, London, 1957, p. 494.
19 F. H. Garner, *Trans. Inst. Chem. Eng. Lond.*, 46 (1950) 275.
20 G. Marrucci, *Chem. Eng. Sci.*, 24 (1969) 975.
21 S. Hartland, *Chem. Eng. J.*, 1 (1970) 67.
22 J. S. Stefan, *Akad. Wiss. Wien, Math.-Naturwiss Kl.*, 69 (1874) 713.
23 O. Reynolds, *Philos. Trans. R. Soc. (Lond.)*, A177 (1886) 157.
24 Taylor, see W. Hardy and I. Bircumshaw, *Proc. R. Soc. Lond.*, A108 (1925) 12.
25 G. E. Charles, R. S. Allan and S. G. Mason, *J. Colloid Sci.*, 16 (1961) 150.
26 G. A. H. Elton and R. C. Picknett, *Proc. II. Int. Congr. Surf. Act. (Lond.), Vol. I*, Butterworths, London, 1957, p. 287.
27 S. P. Frankel and K. J. Mysels, *J. Phys. Chem.*, 66 (1960) 190.
28 D. C. Chappelear, *J. Colloid Sci.*, 16 (1961) 186.
29 G. E. Charles and S. G. Mason, *J. Colloid Sci.*, 15 (1960) 235.
30 H. Brenner, *Chem. Eng. Sci*, 16 (1961) 242.
31 A. D Maude, *Br. J. Appl. Phys.*, 12 (1961) 293.
32 G. D. M. Mackay, M. Suzuki and S. G. Mason, *J. Colloid Sci.*, 18 (1963) 103.
33 G. V. Jeffreys and J. L. Hawksley, *A. I. Chem. Eng. J.*, 11 (1965) 413.
34 G. B. Lawson, *Chem. Process Eng.*, 47 (1967) 45.